Large-eddy simulations of conjugate heat transfer over iced surfaces

FEDERICO ZABALETA

CENTER FOR TURBULENCE RESEARCH, STANFORD UNIVERSITY

Advanced Modeling and Simulation (AMS) Seminars Series

NASA Ames Research Center, January 29, 2026







Introduction to aircraft icing

What is Aircraft Icing?

Occurs when supercooled water droplets freeze on aircraft surfaces. Requires:

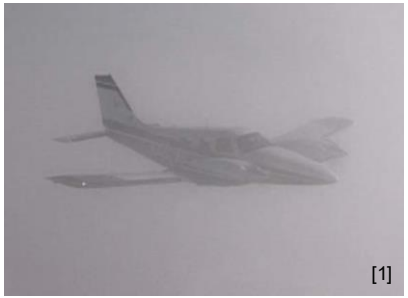
- Temperature below 2°C
- Sufficient airborne moisture



Relevance

Aircraft icing is important to safety and certification reasons:

- 800 accidents between 1982-2000 related to icing (50% fatal).
- Complex verification for new geometries



Aircraft flying in icing conditions



Ice build-up on wing leading edge

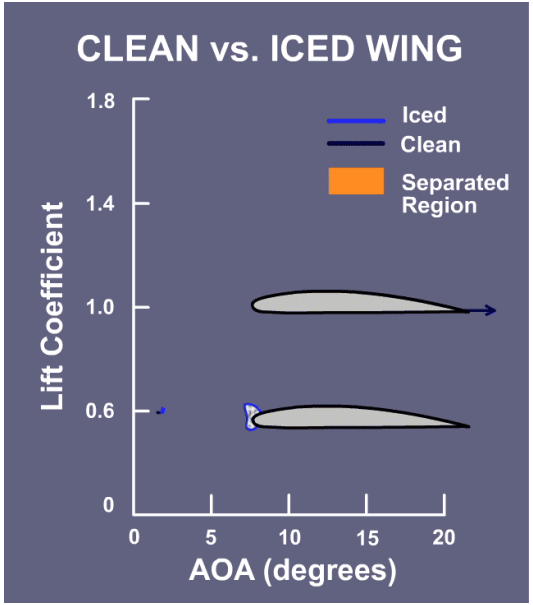


West Wind Aviation Flight 282 from Fond-du-Lac Airport, Canada. 12/13/2017

[1] - https://aircrafticing.grc.nasa.gov/
[2] - Aircraft Technical Book Company

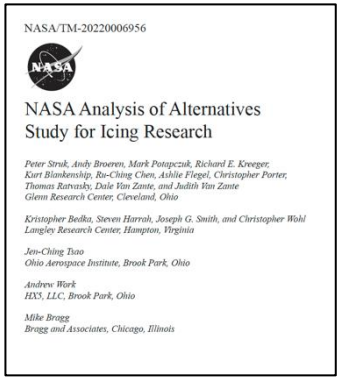
Introduction to aircraft icing

- Aircraft icing impacts airplane performance and is a consideration for certification and safety analysis.
- Two FAA Rule Changes (App. C, D, and O):
  - 2007 – Explicit requirements for handling/performance in both icing and non-icing conditions.
  - 2014 – Extended certification envelope for supercooled large droplets (SLD)
- Ice on wings introduces challenges for simulations:
  - Complex geometries for body-fitted meshes
  - Additional scales due to rough surfaces
  - Ice accretion modeling (droplet splashing, runback, freezing)



Source: https://aircrafticing.grc.nasa.gov/

Certification



NASA/TM-20220006956

NASA Analysis of Alternatives Study for Icing Research

Peter Struk, Andy Broeren, Mark Potapczuk, Richard E. Kreeger, Kurt Blankenship, Ru-Ching Chen, Ashlie Flegel, Christopher Porter, Thomas Ratvasky, Dale Van Zante, and Judith Van Zante
Glenn Research Center, Cleveland, Ohio

Kristopher Bedka, Steven Harrah, Joseph G. Smith, and Christopher Wohl
Langley Research Center, Hampton, Virginia

Jen-Ching Tsao
Ohio Aerospace Institute, Brook Park, Ohio

Andrew Work
HX5, LLC, Brook Park, Ohio

Mike Bragg
Bragg and Associates, Chicago, Illinois

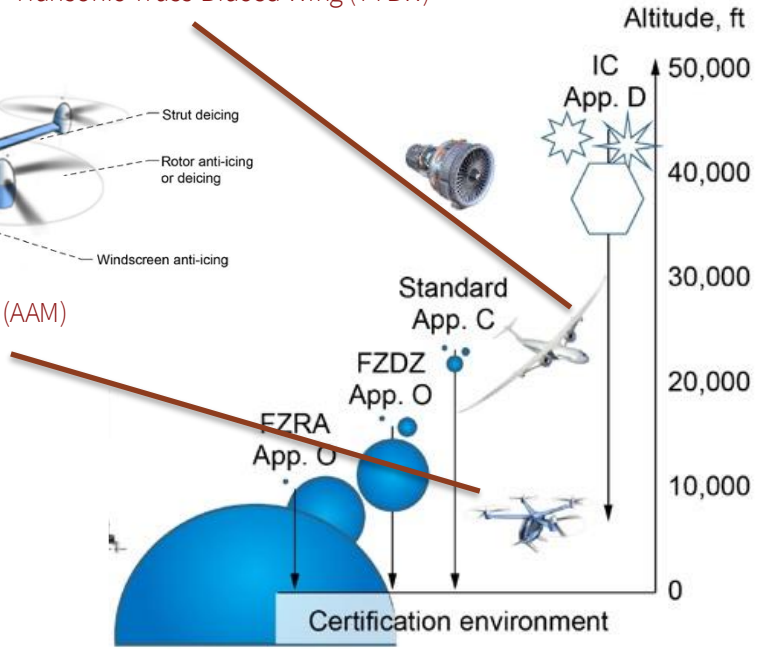
"The current situation relative to new regulations is that **manufacturers greatly rely on similarity to existing designs**, fleet history, and experience. The new regulations could limit research and development toward new and different designs.."



Transonic Truss-Braced Wing (TTBW)



Advanced Air Mobility (AAM)



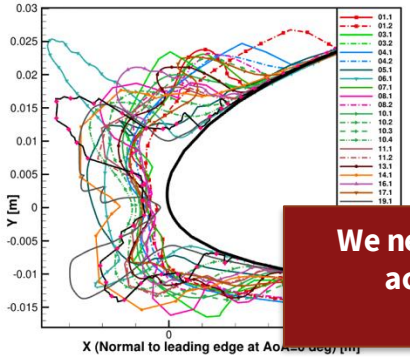
CTR Stanford University
CENTER FOR TURBULENCE RESEARCH

Certification

1

Given flight and atmospheric conditions, we need tools to predict ice growth (shape)

Laurendeau et al. (2022). Summary from the 1st AIAA Ice Prediction Workshop, in: AIAA AVIATION 2022 Forum. American Institute of Aeronautics and Astronautics.

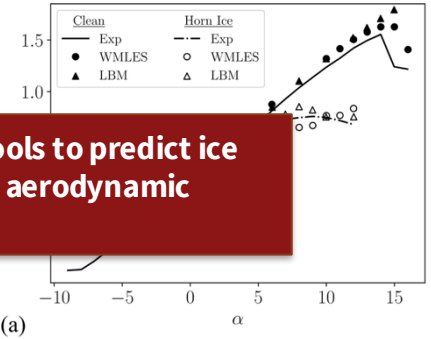


NACA23012 (Case 242-1 IPW)

2

Given an ice shape, we need models to predict aerodynamic degradation

Bornhoft et al. (2022). CTR Annual Research Briefs.
Bornhoft et al. (2023). SAE Technical Paper.
Bornhoft et al. (2024). Aerospace Science and Technology
Penner et al. (2024). AIAA Aviation.
Wong et al. (2024). AIAA Aviation.
Bornhoft et al. (2025). Journal of Aircraft.
Penner et al. (2025). NASA/TM–20250010570



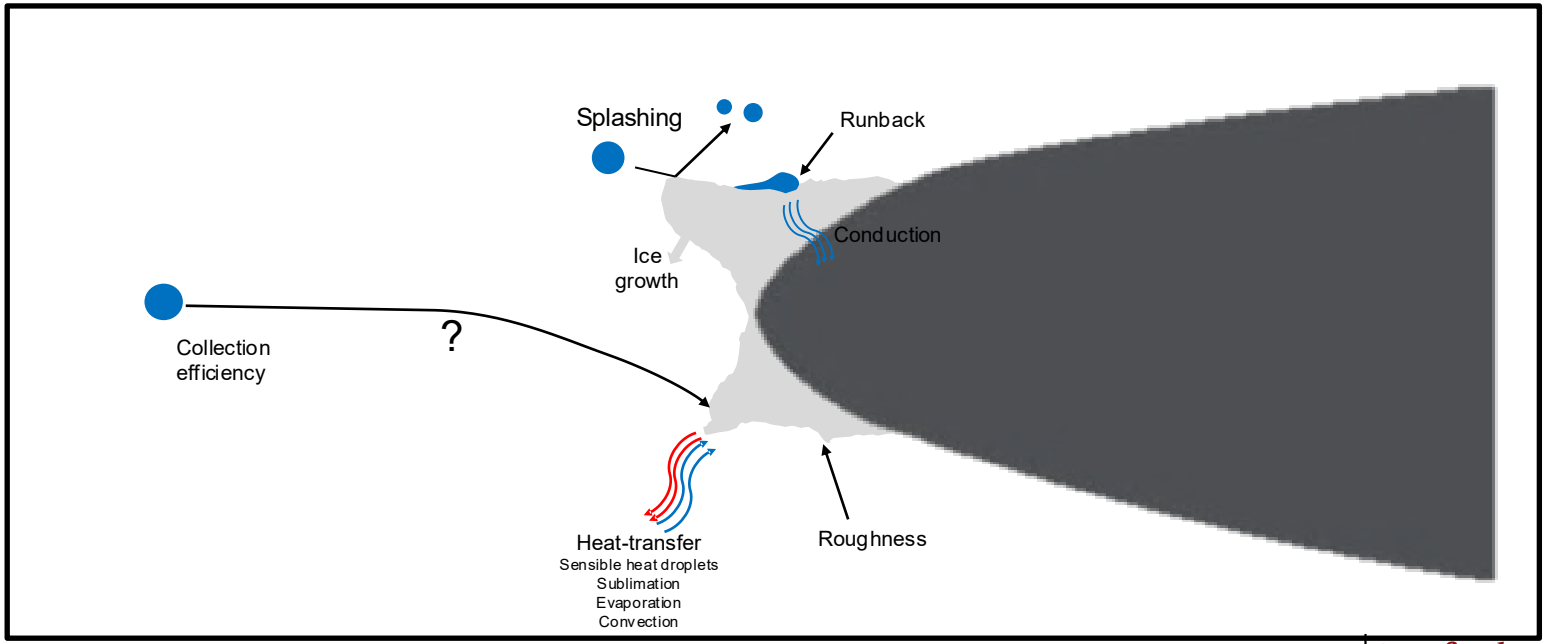
We need validated modeling tools to predict ice accretion and the resulting aerodynamic degradation!

Outline

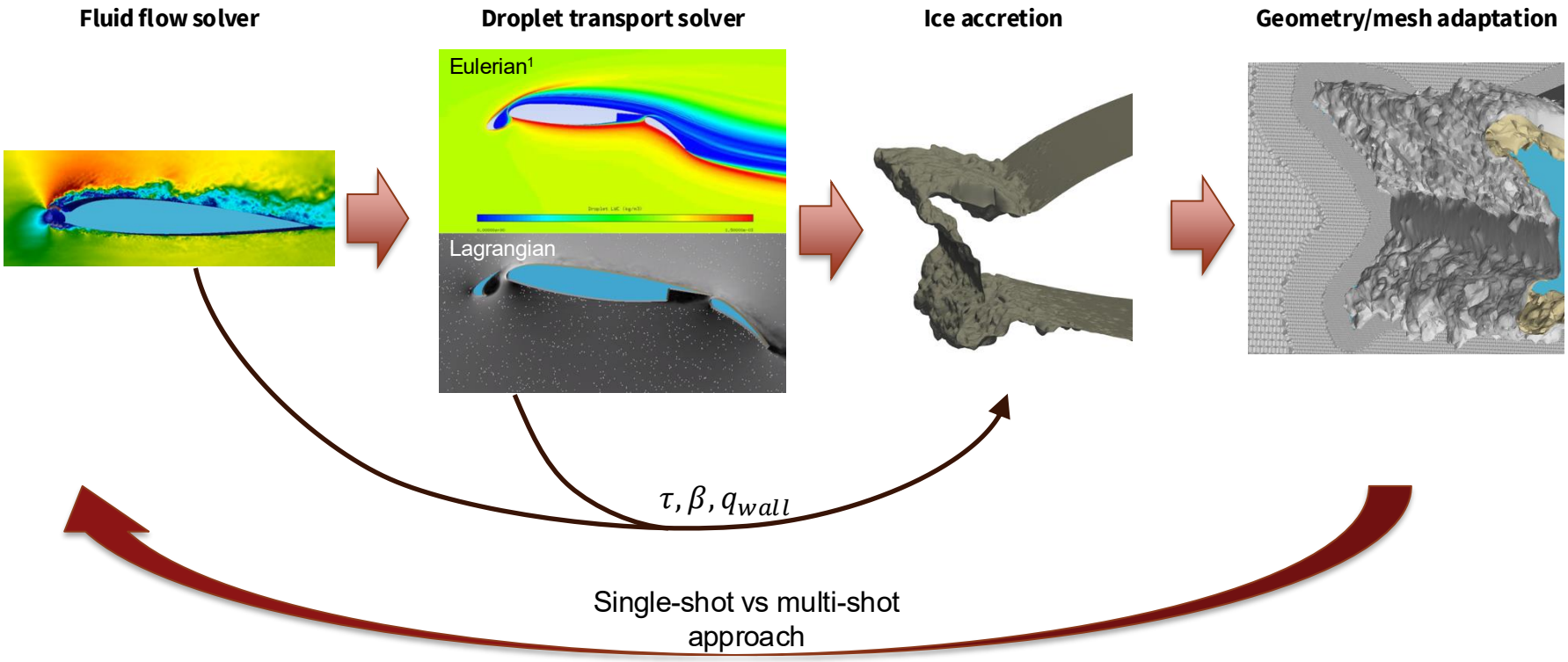
- Background
  - Intro to aircraft icing
  - Certification under new FAA rules
- Evaluation of WMLES for the prediction of heat-transfer in boundary layers over laser-scanned ice roughness
  - Methodology
  - Validation
  - Role of conduction on convective heat-transfer
- Roughness characterization of ice roughness
- Heat-transfer under realistic icing conditions
  - Droplet impingement
  - Heat-transfer on iced airfoils

Ice accretion prediction: a multiphysics problem





Traditional ice accretion modeling

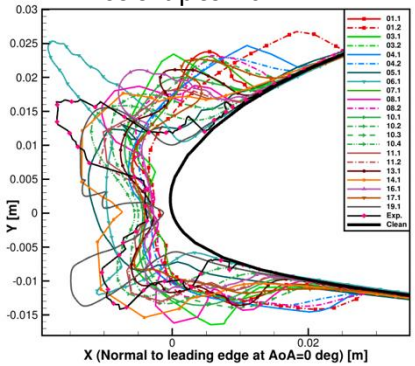


[1] Moula, G. and Ozcer, I., 2023, doi:10.4271/2023-01-1478.

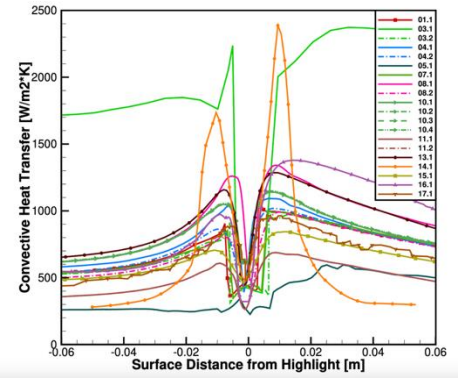
Role of heat transfer

- The formation of ice in glaze conditions depends on a balance of Latent Heat of solidification, Convection and Conduction

Ice shapes from IPW1



Convective HT from IPW1



- Sensitivity analysis has demonstrated that ice shape is highly affected by heat flux variations
- Motivates the study of heat transfer in rough surfaces

Experiments from McCarrel et al. (2018)

Objectives:

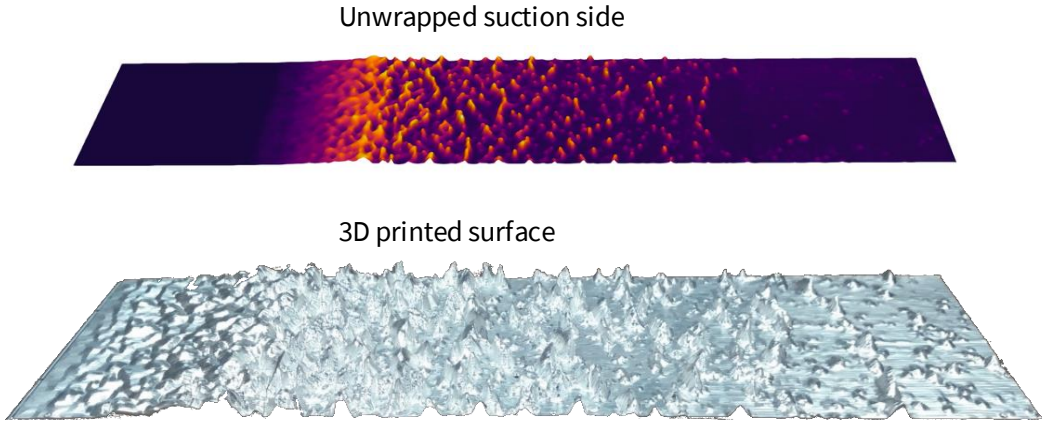
- Evaluate WMLES for heat transfer in rough-surfaces, create best practices, and identify modeling gaps.
- Validate our approaches by comparing to experimental data.

Evaluation of heat transfer on rough surfaces using WMLES:

- Experiments of boundary layer with ice roughness from McCarrel et al. (2018)
- 21-in. NACA 0012 airfoil exposed to supercooled large droplet (SLD) conditions

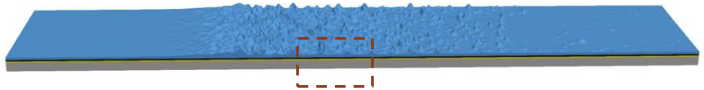


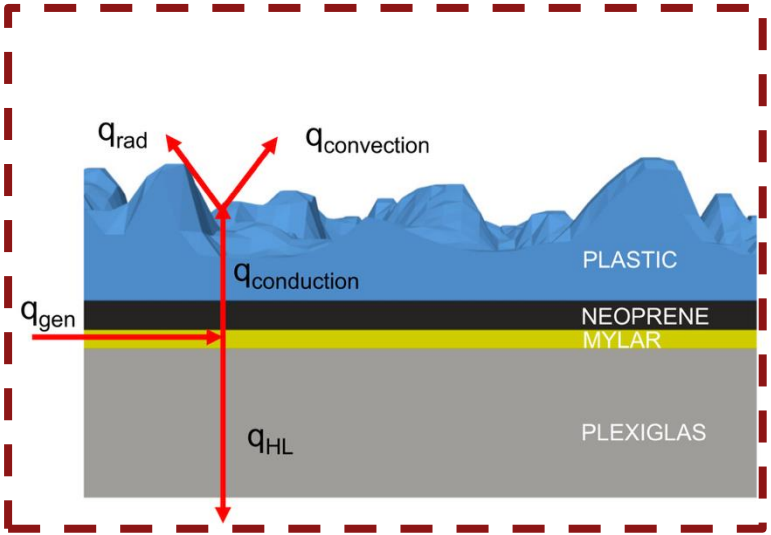


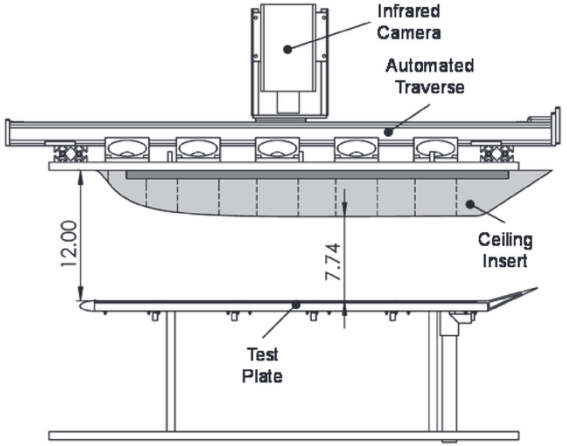


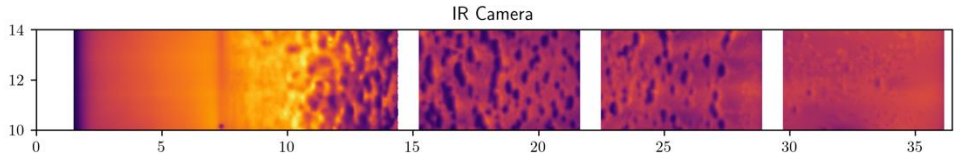
Experimental setup

- IR Camera (±1.4K)
- ZPG Boundary Layer
- No tripping
- $Q_{gen} \approx 550 \pm 27\ W/m^2$









Validation experiment from McCarrel et al. (2018)

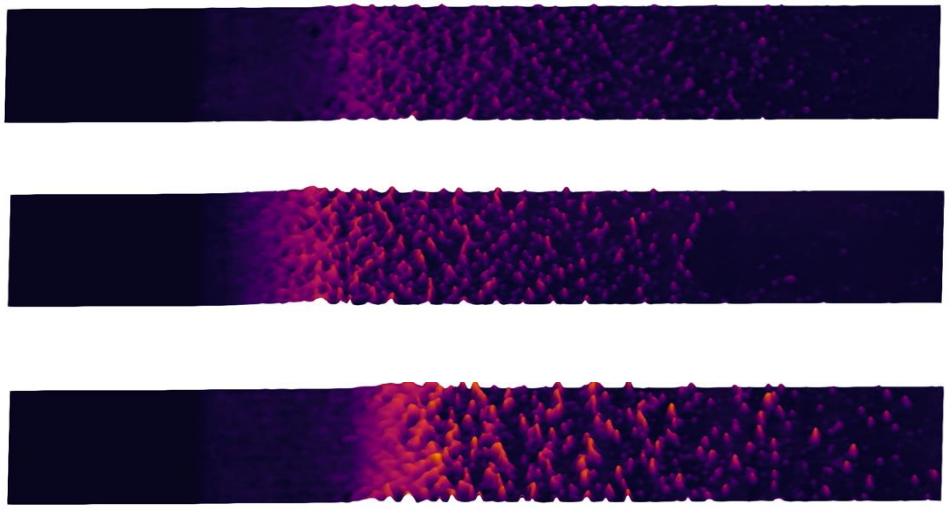
Three surfaces for different exposure times were tested:

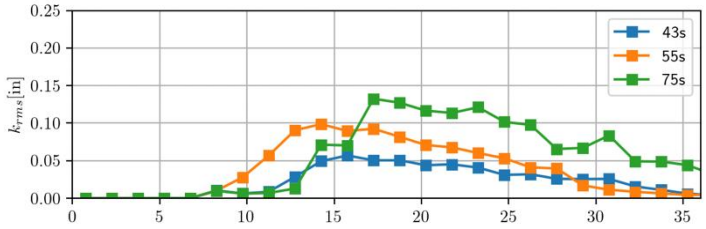
- Different realizations of the experiments.
- As exposure time increases, maximum roughness height increases as well

Three surfaces for different exposure times

Case Identifier	T_t (°C)	T_t (°F)	V (knots)	MVD (μm)	LWC (gm/m^3)	Δt_s (s)
113012.05	-2.43	27.7	129.7	150	0.6	43
112912.02	-2.37	27.8	129.7	100	0.6	55
113012.04	-2.43	27.7	129.7	150	0.6	75

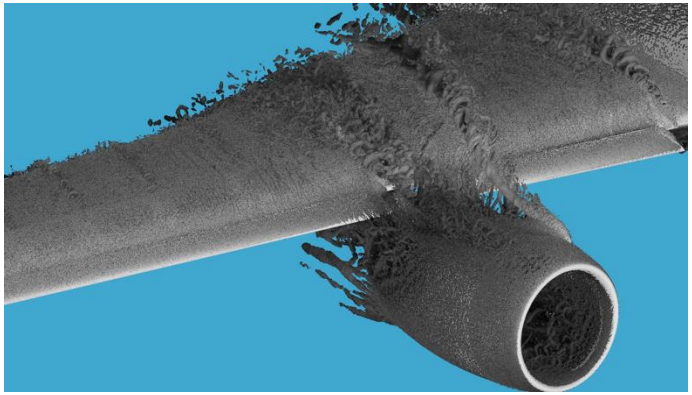
Unwrapped suction side
(colored by elevation)





WMLES: charLES with CHT

- 2nd order finite-volume method, **low-dissipation numerics**
- Kinetic Energy and Entropy Preserving (**KEEP**)
- **GPU Accelerated**



Fluid domain: Compressible Navier-Stokes Equations

$$\frac{\partial \overline{\rho}}{\partial t} + \frac{\partial \overline{\rho}\tilde{u}_i}{\partial x_i} = 0,$$

$$\frac{\partial \overline{\rho}\tilde{u}_i}{\partial t} + \frac{\partial \overline{\rho}\tilde{u}_i\tilde{u}_i}{\partial x_i} = -\frac{\partial \overline{p}}{\partial x_i} + \frac{\partial \tilde{\tau}_{ij}}{\partial x_i} - \frac{\partial \tilde{\tau}_{ij}^{\mathrm{sgs}}}{\partial x_i},$$

$$\frac{\partial \overline{E}}{\partial t} + \frac{\partial \tilde{u}_i\overline{E}}{\partial x_i} + \frac{\partial \tilde{u}_i\overline{p}}{\partial x_i} = \frac{\partial \tilde{\tau}_{ij}\tilde{u}_i}{\partial x_i} - \frac{\partial \tilde{\tau}_{ij}^{\mathrm{sgs}}\tilde{u}_i}{\partial x_i} + \frac{\partial}{\partial x_i}\left(\lambda\frac{\partial \overline{T}}{\partial x_i}\right) - \frac{\partial \tilde{Q}_i^{\mathrm{sgs}}}{\partial x_i},$$

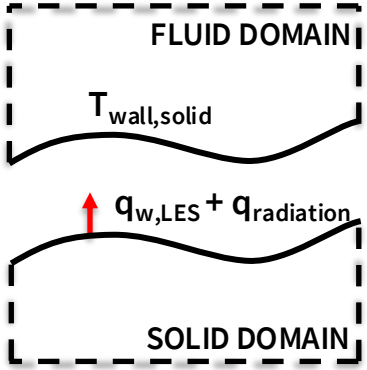
Solid domain: Heat equation

$$\frac{\partial \rho_s c_{p,s} T}{\partial t} + \frac{\partial}{\partial x_j}\left(\lambda_s\frac{\partial T}{\partial x_j}\right) = 0,$$

Interface fluid-solid

$$\lambda_s \left.\frac{\partial T}{\partial n}\right|_w = q_{w,\mathrm{LES}} + q_{\mathrm{radiation}}$$

$$q_{\mathrm{radiation}} = \sigma\epsilon(T_w^4 - T_\infty^4)$$



Closures:

- Dynamic Smagorinsky
- Eq. wall model (turbulent portion)
- Blasius wall-model (laminar portion)

Why CHT?

The Biot number compares the internal thermal resistance due to conduction within a solid to the external resistance due to convection at its surface

$$\mathrm{Bi} = \frac{hL}{\lambda_s}$$

h: Heat transfer coefficient
λ_s: Thermal conductivity solid
L: Length-scale (k_z)

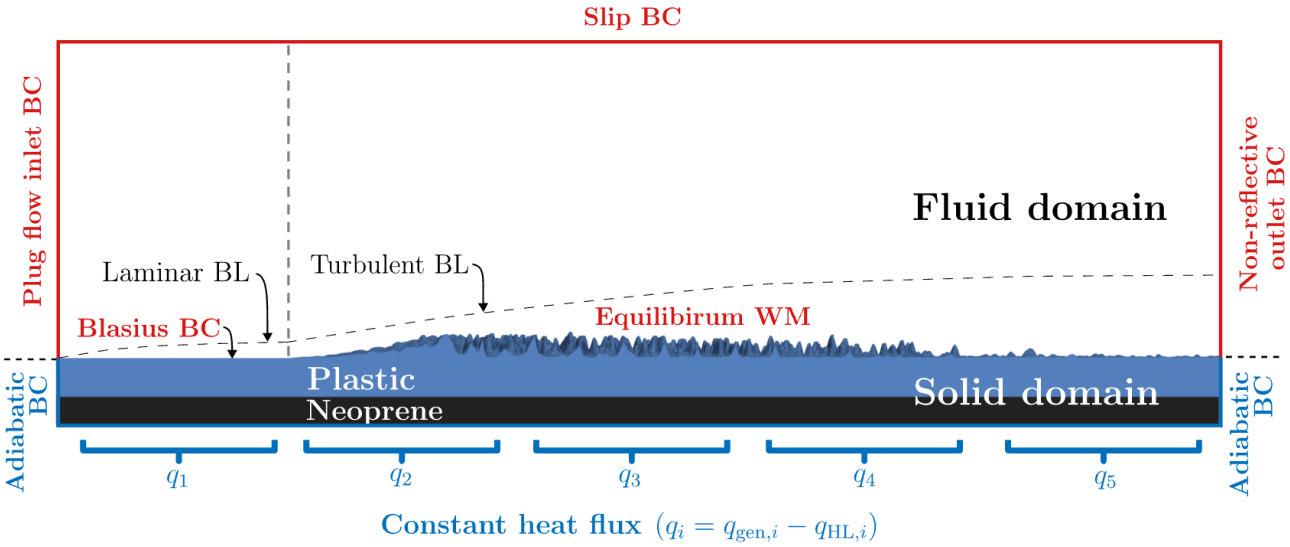
For $\mathrm{Bi} \ll 0.1$, negligible temperature gradients within the solid (isothermal walls)
For $\mathrm{Bi} > 0.1$, temperature gradients become significant

From experiments:

$$\mathrm{Bi} \approx 3$$

$$h = 50\, W/m^2K$$
$$\lambda_s = 0.162\, W/m^2$$
$$k_z = 0.01\mathrm{m}$$

Computational setup



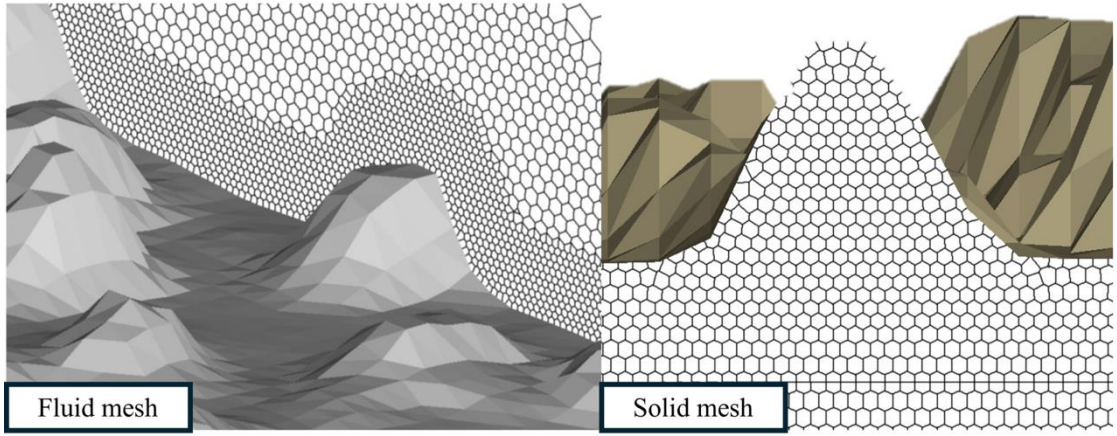
Vertical dimension not to scale

Body-fitted representation of roughness

- Body-fitted mesh based on Voronoi diagrams
- $k_{rms}/\Delta \approx 2$ for medium mesh (similar to work from Bornhoft)

Mesh properties

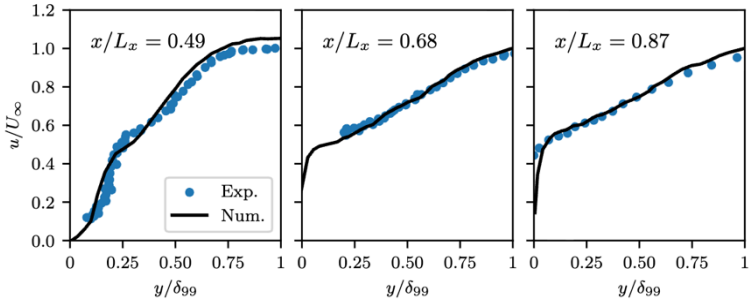
Geometry	Grid	N_{cv} (Mcv) (fluid, solid)	k_{rms}/Δ_{min} (max, mean)	k_z/Δ_{min} (max, mean)	δ_{99}/Δ_{min} $[(0.1,\ 0.4,\ 0.7)\,L_x]$	y^+ (max, mean)
s43	Coarse	1.5, 0.2	1.1, 0.6	5.6, 3.7	1.9, 8, 17	68, 20
	Medium	6.3, 2.0	2.2, 1.1	11, 7.4	3.9, 15, 34	34, 10
	Fine	25, 15	4.5, 2.3	22, 15	7.7, 30, 67	17, 5
s55	Coarse	1.6, 0.2	1.9, 0.9	7.9, 5.7	1.9, 13, 22	68, 20
	Medium	6.6, 1.9	3.7, 1.8	16, 11	3.9, 27, 44	34, 10
	Fine	27, 16	7.5, 3.6	32, 23	7.7, 54, 88	17, 5
s75	Coarse	1.7, 0.2	2.6, 1.3	11, 7.3	1.9, 10, 24	70, 22
	Medium	6.9, 2.2	5.2, 2.6	21, 15	3.9, 19, 49	35, 11
	Fine	28, 17	11, 5.2	42, 29	7.7, 38, 97	17, 6



Validation

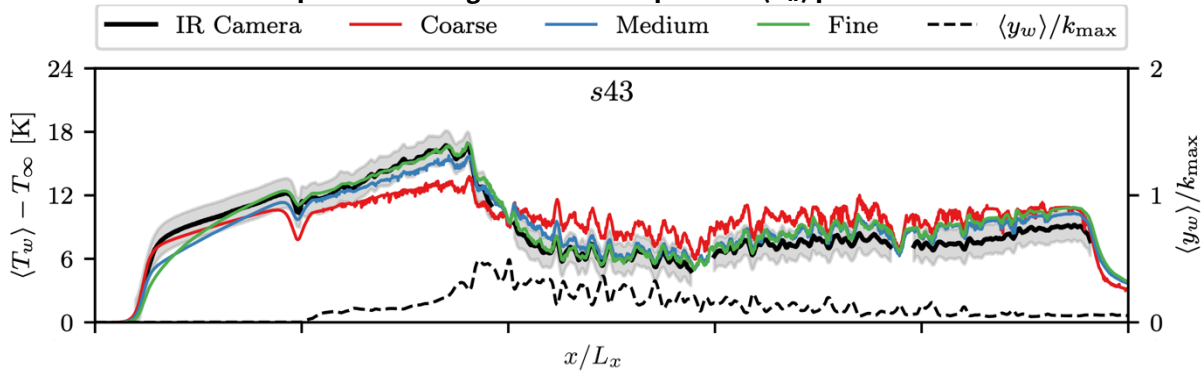
- Velocity profiles closely match experiments.
- Computed temperatures fall within the experimental uncertainty (±1.4 K) for most of the domain.
- Medium and Fine meshes show identical results in the rough region

Velocity profiles



Spanwise averaged surface temperature (T_w) profiles

T_{ice} = 43s

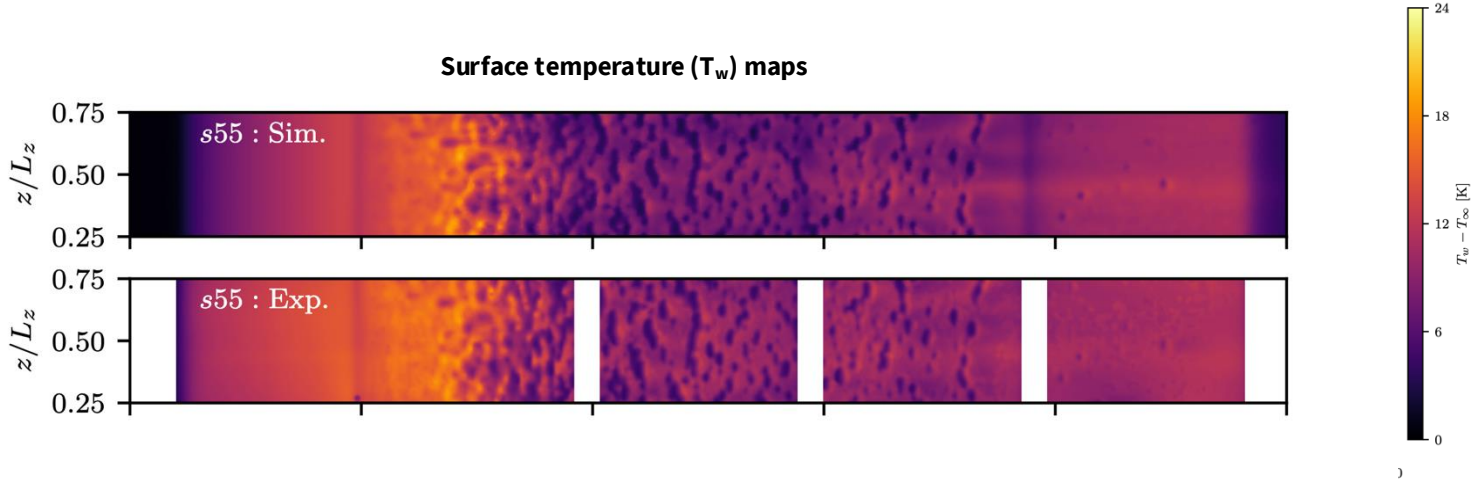


CTR Stanford University
CENTER FOR TURBULENCE RESEARCH

Validation

- The simulation successfully captures local temperature maxima and minima in the rough region.
- Low temperature at roughness peaks, higher temperature at valleys

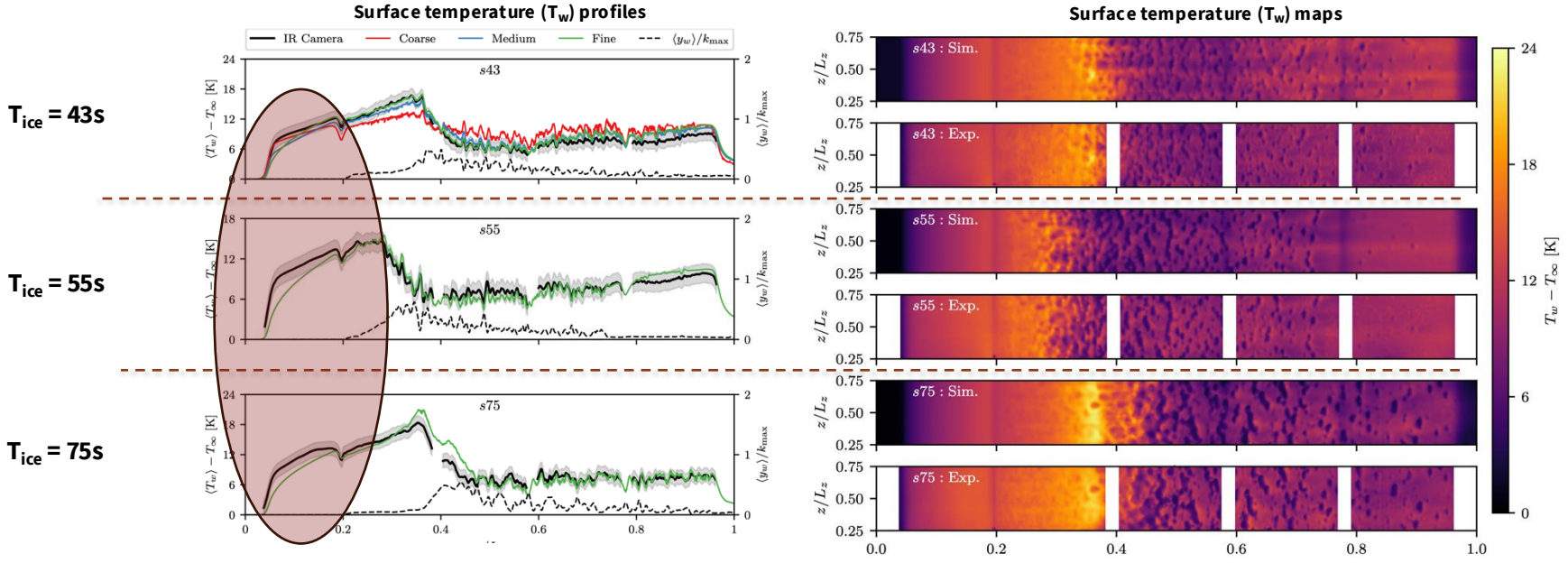
T_{ice} = 43s



CTR Stanford University
CENTER FOR TURBULENCE RESEARCH

Validation

- Computed temperatures profiles for all geometries fall within the experimental uncertainty (±1.4 K) for most of the domain.
- Discrepancy between simulations and experiments in the laminar region due to underresolution.

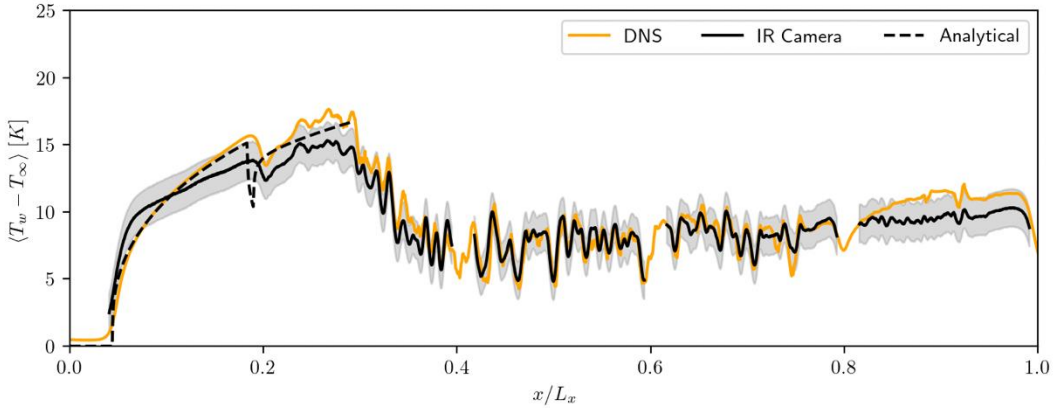


Laminar BL

- There is an analytical expression of the temperature distribution in a laminar boundary layer with an unheated start

$$T_0(x) - T_\infty = \frac{0.623}{k} \mathrm{Pr}^{-1/3} \mathrm{Re}_x^{-1/2} \int_{\xi=0}^{x} \left[1 - \left(\frac{\xi}{x} \right)^{3/4} \right]^{-2/3} q''(\xi)\, d\xi$$

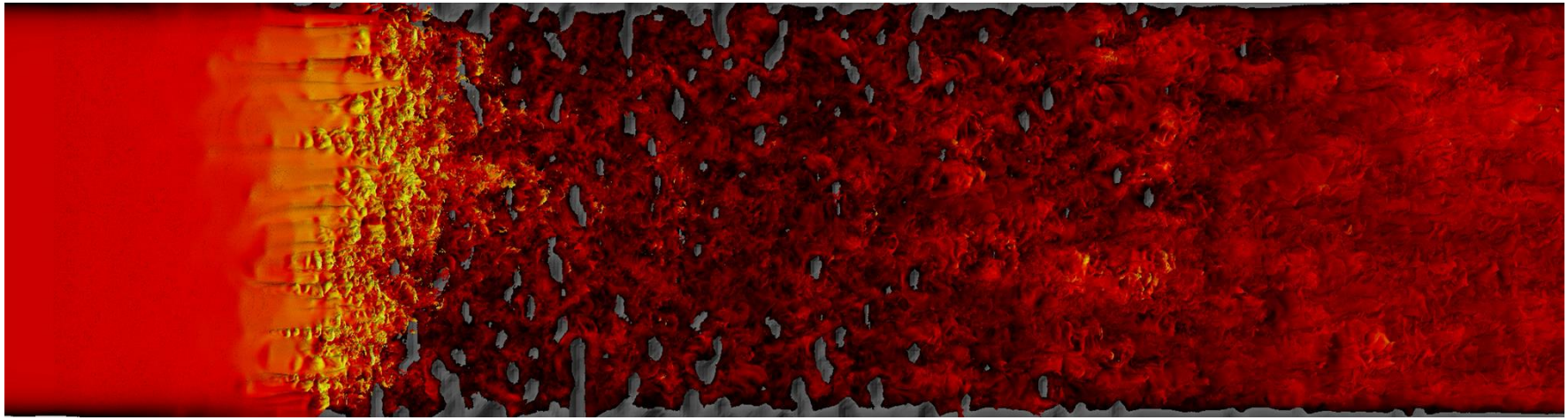
- We performed DNS simulations of the present geometry to understand the effect of the laminar BL and of transition
- Discrepancies in the first “unheated gap” due to lateral conduction in the solid



Laminar BL

- Transition triggered from the interaction with first rough elements.
- Elongated wakes transition, departing from the analytical solution.
- Discrepancies in the first “unheated gap” due to lateral conduction in the solid

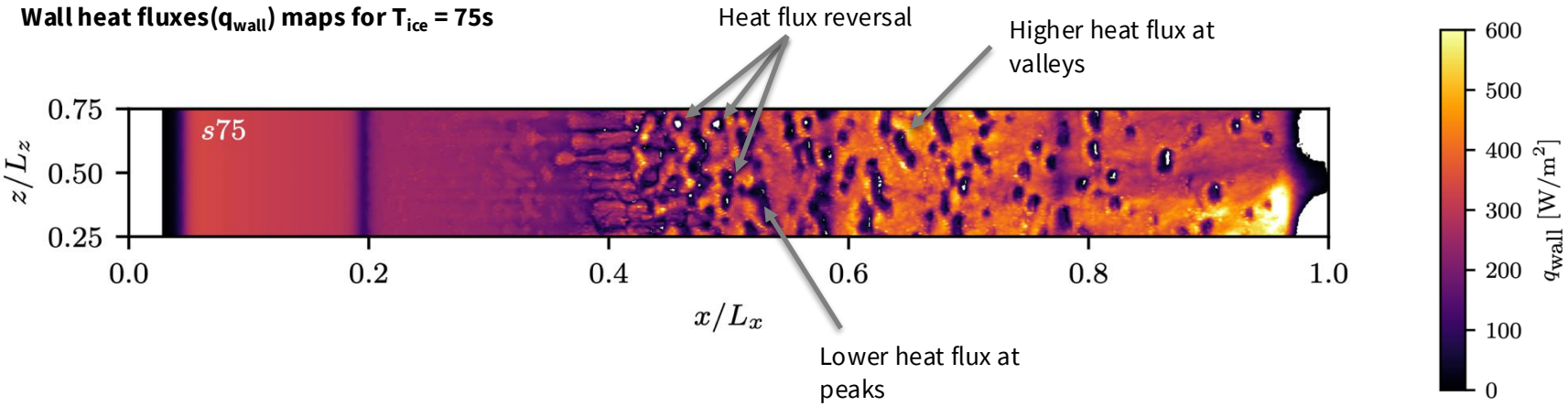
Iso-surfaces of $\mathbf{T = 299\ K}$ colored by velocity magnitude



Heat-fluxes calculations

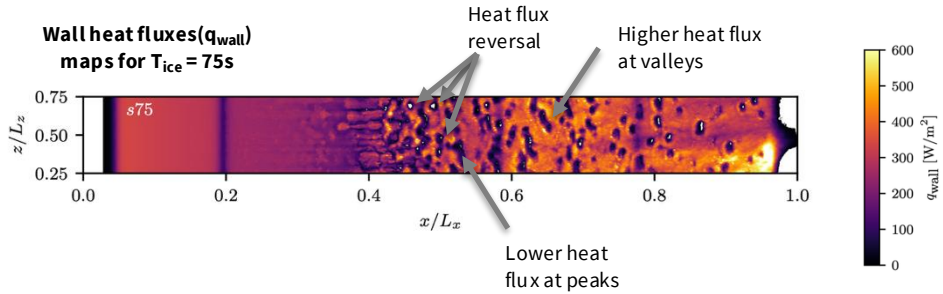
- Roughness increases heat fluxes
- Heat flux maps show higher heat fluxes at roughness valleys and lower at peaks.

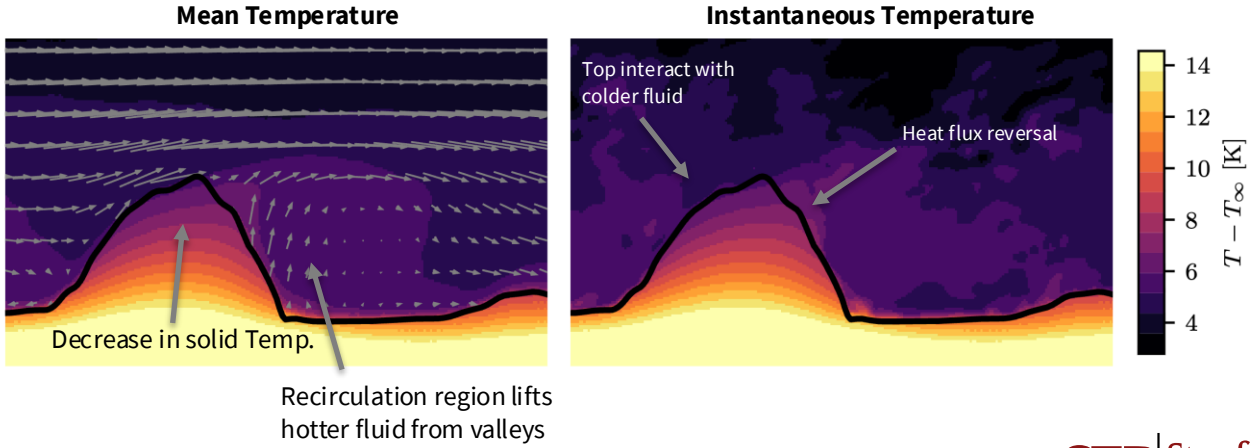
Wall heat fluxes(q_{wall}) maps for T_{ice} = 75s



Heat-fluxes calculations

- Roughness elements temperature decreases from base to peak
- Recirculation behind roughness peaks lifts higher temperature fluid towards the back of the roughness elements.
- Reversal of heat flux happens due to interaction of hotter fluid with colder roughness peaks



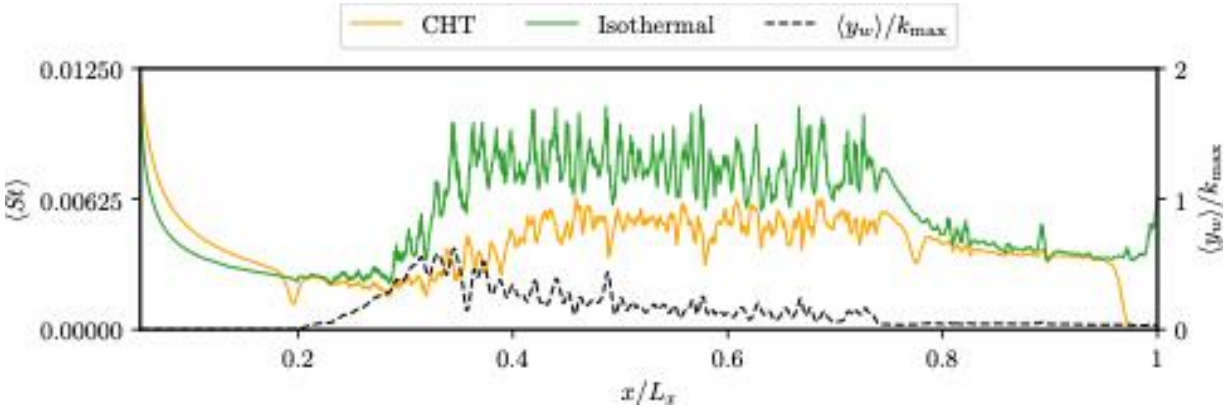


CTR Stanford University
CENTER FOR TURBULENCE RESEARCH

Importance for icing

- For icing applications, heat transfer is usually estimated using isothermal walls.
- Isothermal walls assume materials of infinite conductivity, and it breaks down for low-conductivity materials (plastic, ice)
- Isothermal wall simulations are performed using the same mesh and setup as the CHT simulations, but using uniform T_w, equal to the mean temperature obtained from the CHT model.

$$St = \frac{q_{wall}}{\Delta T \rho c_p U_\infty}$$



- Isothermal simulations lead to a **50% increase** in Stanton number

For ice accretion predictions, CONDUCTIONS MATTERS!

Roughness characterization

Roughness characterization

In ice accretion predictions, roughness is typically described using an equivalent sand grain roughness (k_s) or the roughness function (ΔU).

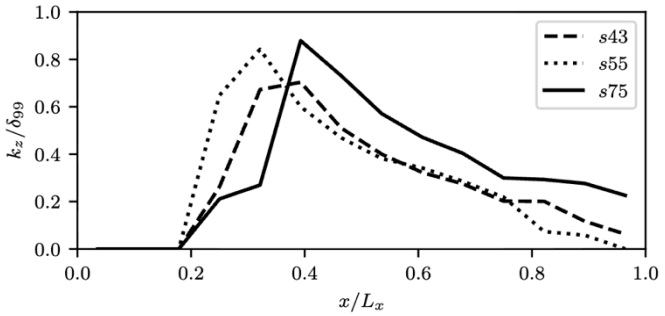
$$U^+ = \frac{1}{\kappa}\ln\left(\frac{y^+}{k_s^+}\right) + B$$

$$U^+ = \frac{1}{\kappa}\ln\left(y^+\right) + C - \Delta U^+$$

These two parameters are equivalent

$$\Delta U^+ = \frac{1}{\kappa}\ln(k_s^+) + C - B.$$

The existence of a logarithmic layer requires that $y > y_k$ and $y \ll \delta$ (or $y_k \ll \delta$), where y_k is the height of the roughness sublayer ($y_k \approx 3k_s$). This is associated with $\frac{k}{\delta} < \frac{1}{19}$ to $\frac{1}{7}$ (depends on the author)



CTR Stanford University
CENTER FOR TURBULENCE RESEARCH

Equivalent ks

- Despite the fact that k/δ often exceeds the established limits for the existence of outer-layer similarity, k_s is still widely employed in icing simulations,
- We compute a "equivalent" value of k_s^+ (or ΔU^+) that would yield the same wall shear stress as the actual rough surface

$$\Delta U^+ = \sqrt{\frac{2}{C_{f,S}}} - \sqrt{\frac{2}{C_{f,R}}},$$

- We compare this to k_s^+ obtained from models based on roughness statistics:

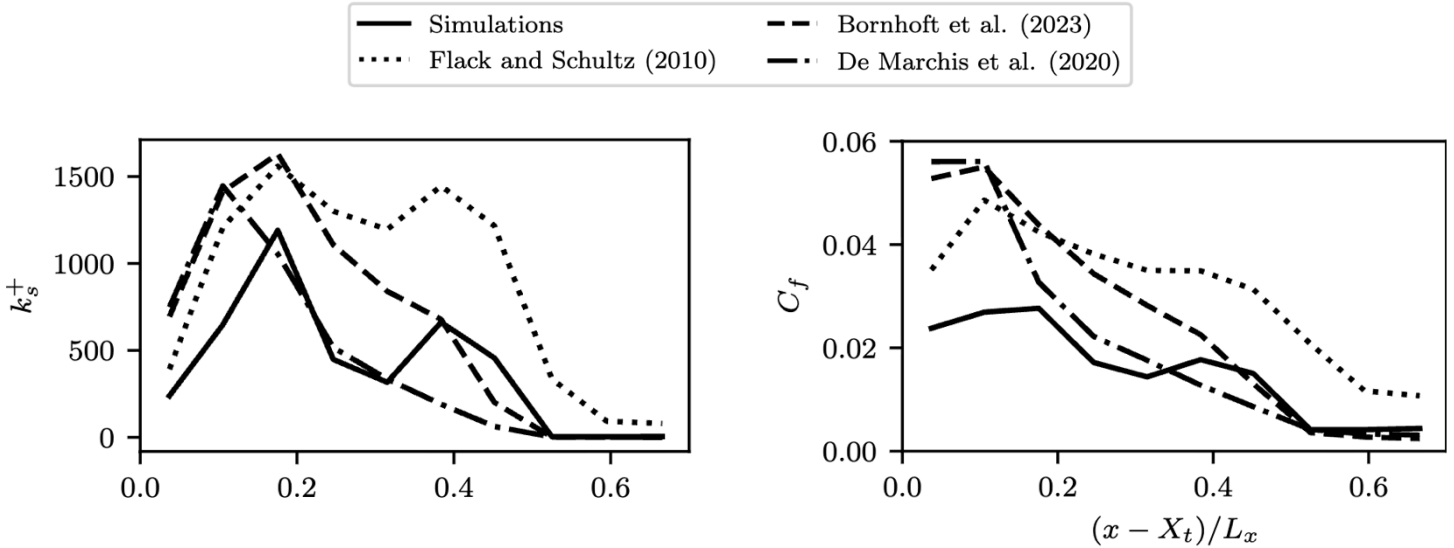
$$k_s^+ = 4.43 k_{\mathrm{rms}}^+ (1 + Sk)^{1.37}$$ Flack and Schultz (2010)

$$\Delta U^+ = c_1 \ln\left(c_2 k_{rms}^+ ES\right) \left[(c_3 - 1)\tanh\left(c_4 s_k\right) + 1\right] e^{-c_5 ES^{c_6}}$$ Bornhoft et al. (2023)

$$\Delta U^+ = \frac{1}{\kappa} \log\left(k_{\mathrm{rms}}^+ ES\right) + 3.5.$$ De Marchis et al. (2020)

Shear-stress prediction by empirical models

- All three models tend to overpredict the values of k_s^+
- The overprediction of k_s^+ leads to an overprediction in C_f



CTR Stanford University
CENTER FOR TURBULENCE RESEARCH

Conclusions

- CHT-WMLES Validation: The Conjugate Heat Transfer (CHT) framework coupled with Wall-Modeled LES accurately predicts surface temperature and heat flux distributions over complex, laser-scanned ice roughness.
- Given the low conductivity of ice, these results suggest that heat flux and temperature variations may play an important role in the formation and development of surface roughness.
- Large roughness-to-boundary-layer thickness ratios disrupt outer-layer similarity, leading to substantial errors in estimating equivalent sandgrain roughness when applying traditional empirical models based on surface statistics

Heat-transfer in Realistic icing conditions

Differences with realistic icing conditions

Main conclusion

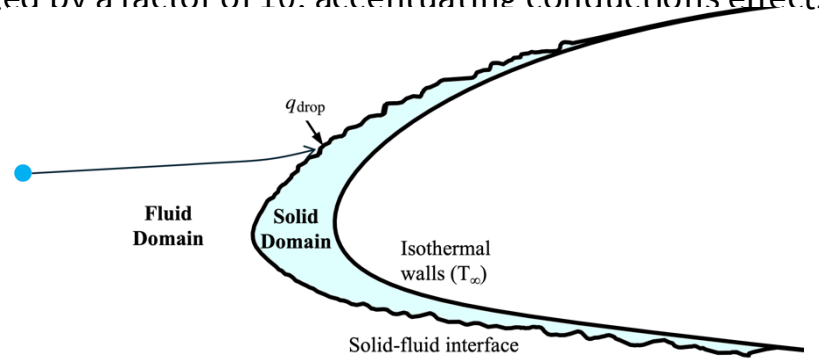
Isothermal simulations lead to a 50% increase in Stanton number. For heat transfer in low conductivity materials (ice), conduction matters.

Differences

1. Heat source was uniform and located at the base of the plate, while in icing conditions heat is generated at the surface.
2. Roughness elements were constructed from ABS plastic, whose thermal conductivity is 10 times smaller than ice thermal conductivity

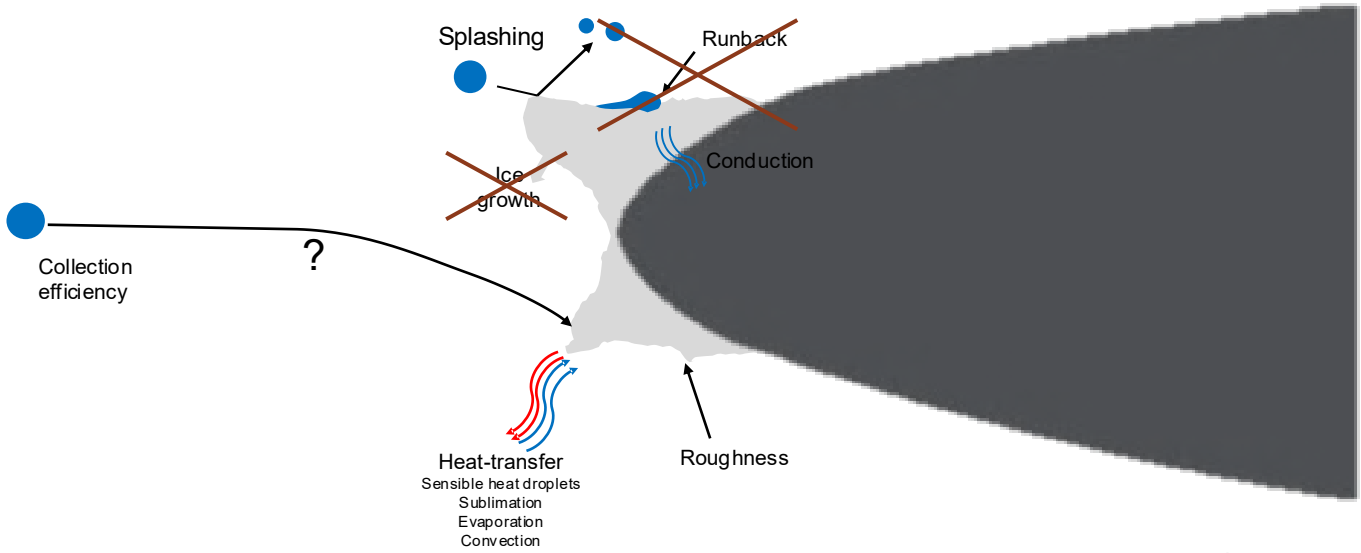
$$k_{ice} = 2\ W/m^2 > 0.2\ W/m^2 = k_{plastic}$$

3. Geometry was scaled by a factor of 10, accentuating conductions effects through its influence in the **Biot number**.



Heat transfer in realistic icing conditions

- Ignore ice growth ($t_{ice} \gg t_{HT}$)
- Ignore water runback (complex thin film dynamics)



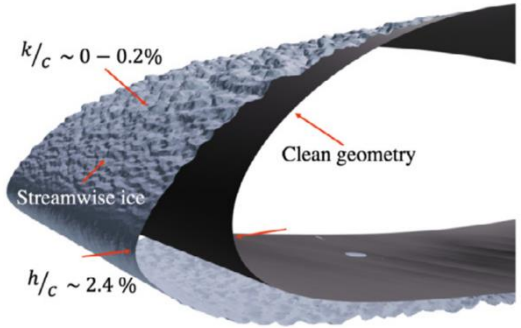
CTR Stanford University
CENTER FOR TURBULENCE RESEARCH

Laser-Scanned Iced NACA23012 Airfoil

ED1977 Streamwise ice from [1]

- $U_\infty = 200$ kt
- $MVD = 30$ μm
- LWC=30 g/m^3
- 7-bin droplet cloud distribution
- 5 min of exposure

Previously studied by Bornhoft et al. [2] to predict aerodynamic degradation







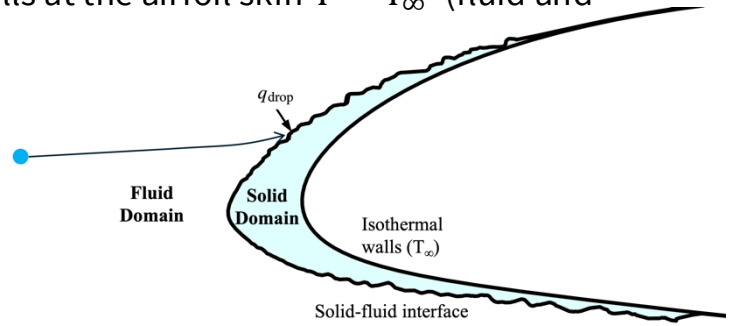
[1] Broeren et al., Journal of Aircraft, 2018
[2] Bornhoft et al., Aerospace Science and Technology, 2024

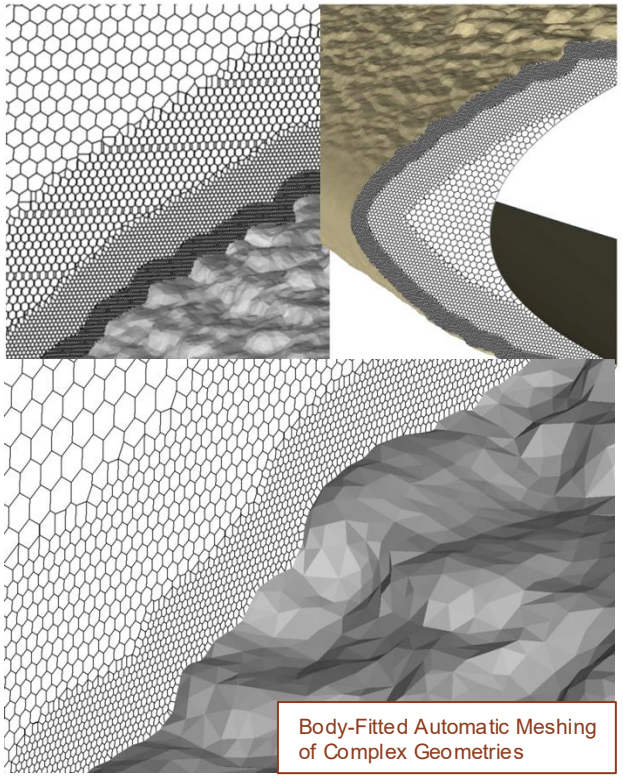
HT on iced airfoils: Computational setup

Simulation procedure:

1. Simulate **flow** around airfoil
2. Inject **particles**, compute β
3. Use steady-state value of β to compute q_{drop} and run the **CHT** solver

- Mesh: 30.4 Mcv (fluid) + 12.1 Mcv (solid)
- DSM + Algebraic wall model
- Isothermal walls at the airfoil skin $T = T_\infty$ (fluid and solid domain)



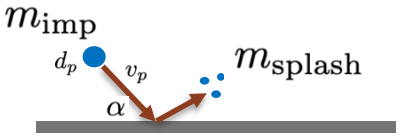


Particle transport solver

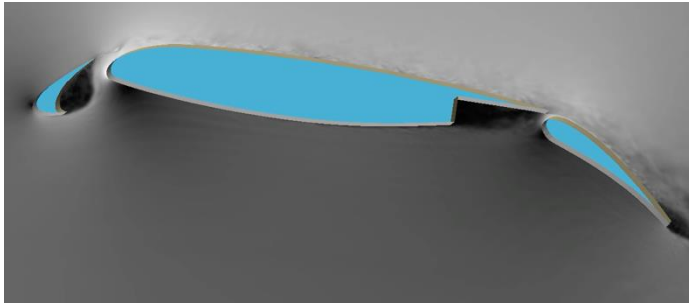
One-way coupled lagrangian particles ($\alpha_d \approx 10^{-6}$)

$$\frac{dx_{p,i}^k}{dt} = u_{p,i}^k \qquad m_p^k \frac{du_{p,i}^k}{dt} = -f_i^k$$

Splashing model by Wright (2008)[1]

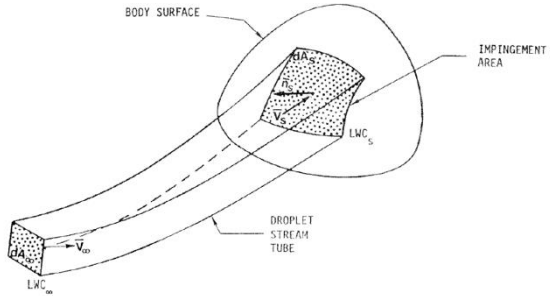


$\uparrow v_p, \uparrow d_p, \downarrow \alpha, \downarrow \text{freq.} \implies$ More splashing



Collection efficiency, β - ratio of the local droplet flux at the body surface to the freestream flux

$$\beta = \frac{m_s}{m_\infty}$$



[1] Wright, William. (2006). https://doi.org/10.2514/6.2006-464.

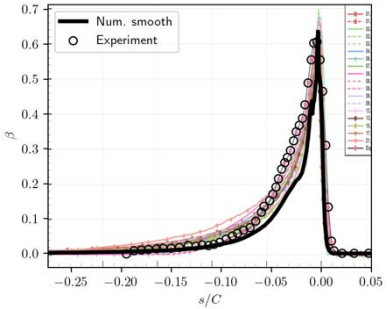
Particle transport solver: Validation

NACA 64A008 swept wing (Papadakis et al. 2002)

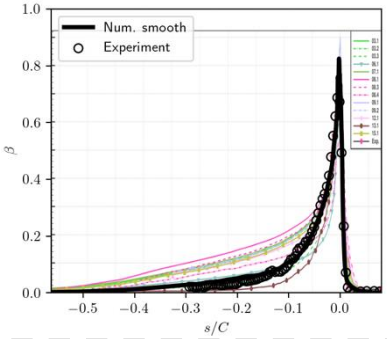
Spray MVD: 21 and 92 microns



MVD 21 microns

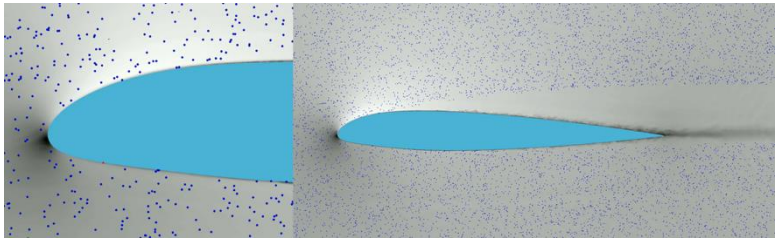


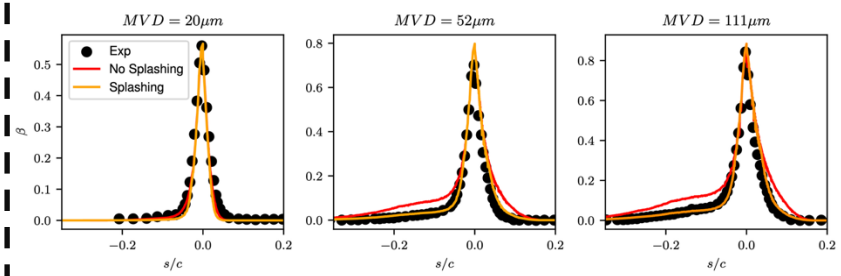
MVD 92 microns



NACA 23012 (Papadakis et al. 2002)

Median Volumetric Diameter: 20µm, 54 µm, 111 µm.

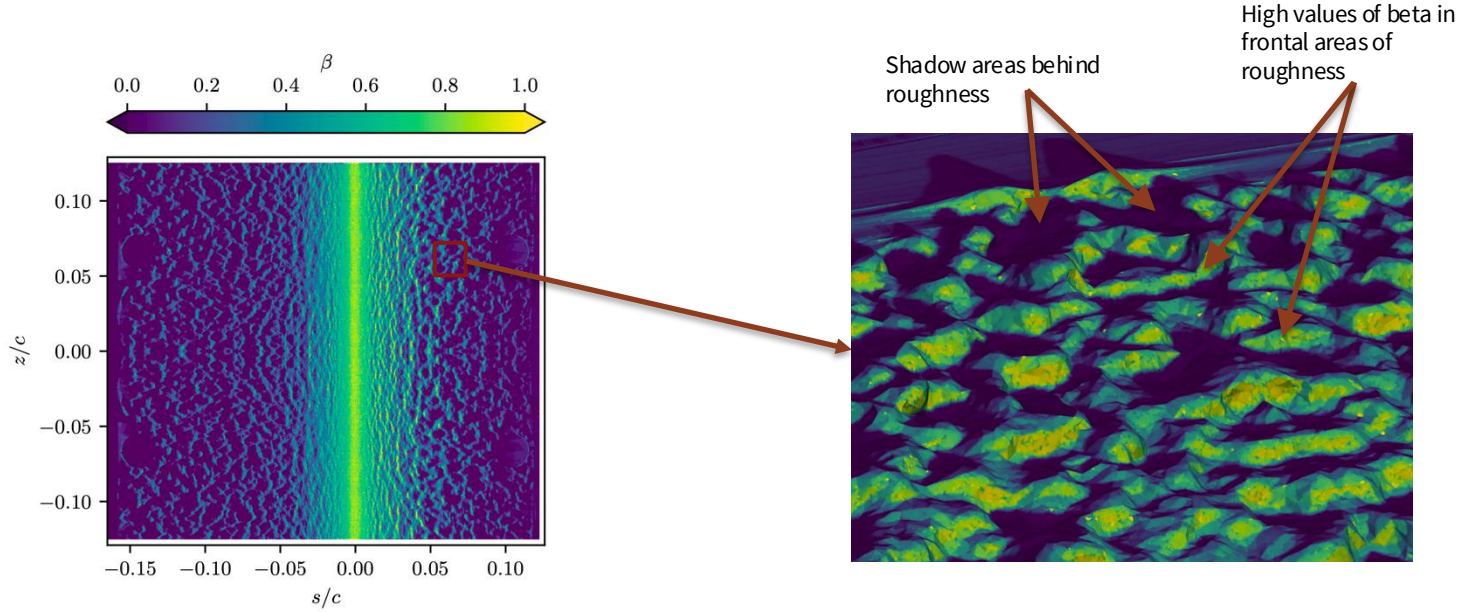




Zabaleta, F., and Moin P.. 2025. "Large-Eddy Simulations of Droplet Impingement on Iced Airfoils." *Annual Research Briefs*, December 1.
Zabaleta et al. 2024. "Large-Eddy Simulation of Supercooled Large Droplets Impingement Using a Lagrangian Particle Approach" AIAA AVIATION FORUM AND ASCEND 2024.

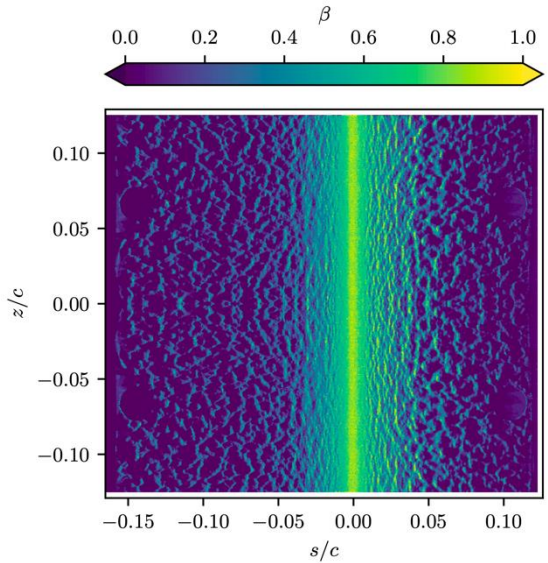
Collection efficiency and heat fluxes in laser-scanned airfoil

- High dispersion of beta in rough region.
- Maximum values of beta on frontal area of roughness elements, shadows zone with almost no impact behind roughness elements.

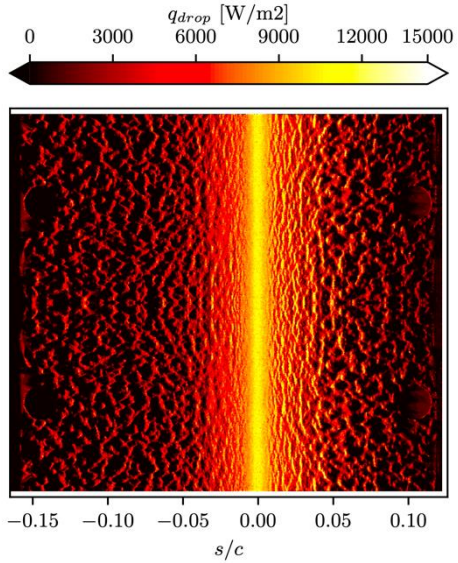


Collection efficiency and heat fluxes in laser-scanned airfoil

- High dispersion of beta in rough region.
- Maximum values of beta on frontal area of roughness elements, shadows zone with almost no impact behind roughness elements.
- Heat source distribution follows the collection efficiency distribution, with some differences in relative magnitude



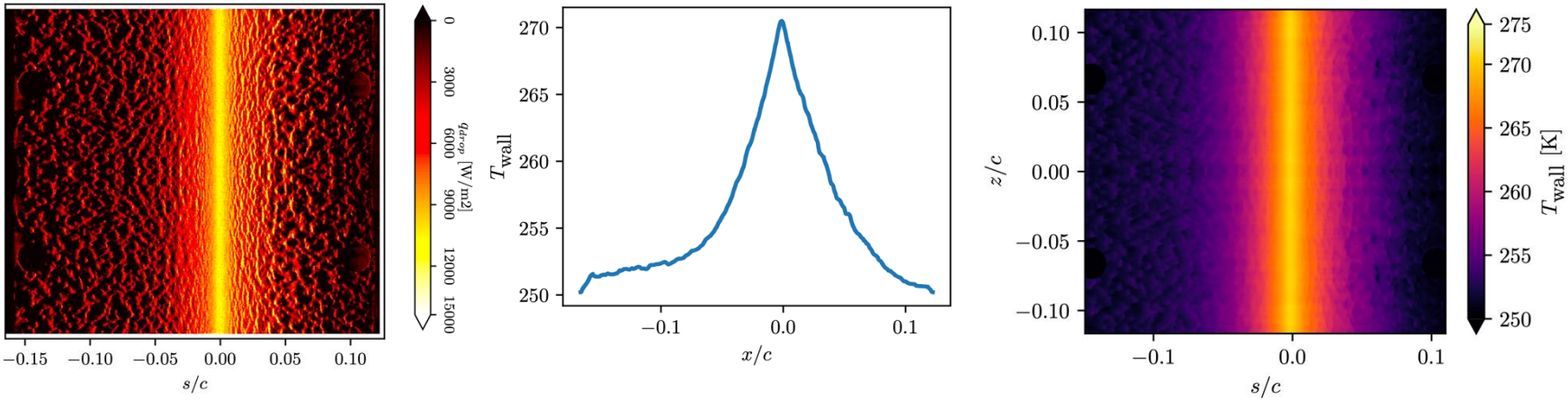
$$q_{\text{drop}} = \text{LWC}\, U_\infty \beta (L_T + (T_d - T_w) c_{p,s})$$



CTR Stanford University
CENTER FOR TURBULENCE RESEARCH

Surface temperature distribution

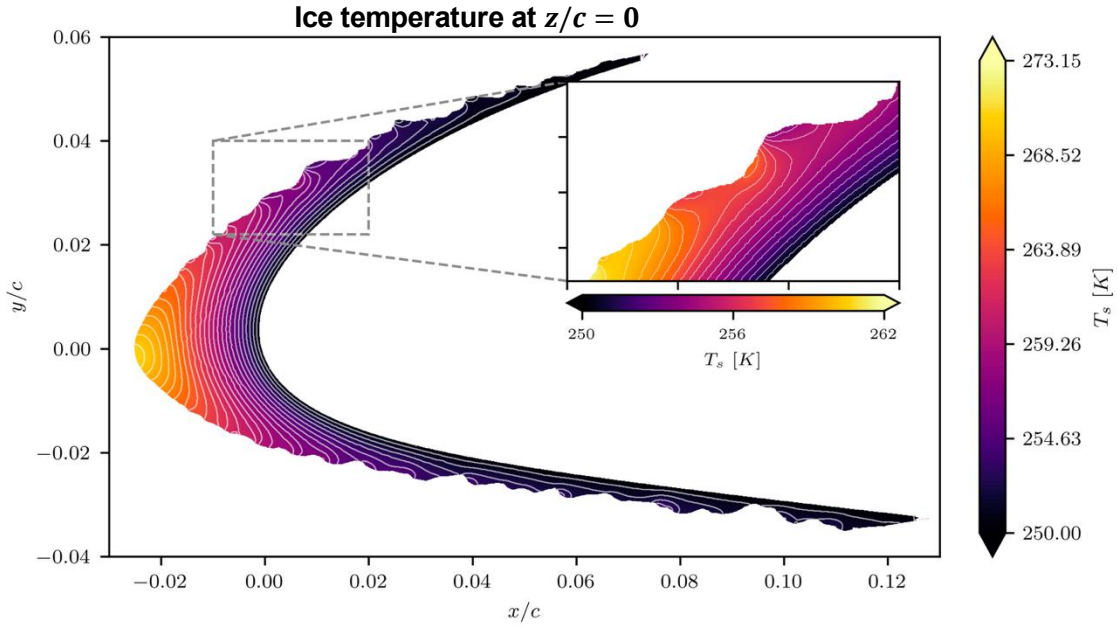
- Maximum temperature at the stagnation line $T_{wall} \approx T_{freezing}$
- Temperature decreases downstream, as ice layer thinks and q_{drop} decreases.
- Local variations arise due to the non-uniform heating. However, temperature gradients are smoother than heating variations



CTR Stanford University
CENTER FOR TURBULENCE RESEARCH

Temperature distribution within the ice layer

- Near the airfoil skin, isotherms are parallel to the wall, indicating one-dimensional conductive heat transfer.
- Near the ice surface, isotherms curve and intersect the the ice surface, showing an important component of lateral conduction.
- The windward faces of roughness elements show higher temperatures than on the leeward faces.
- These local variations lead to important heat-conduction through the roughness elements.

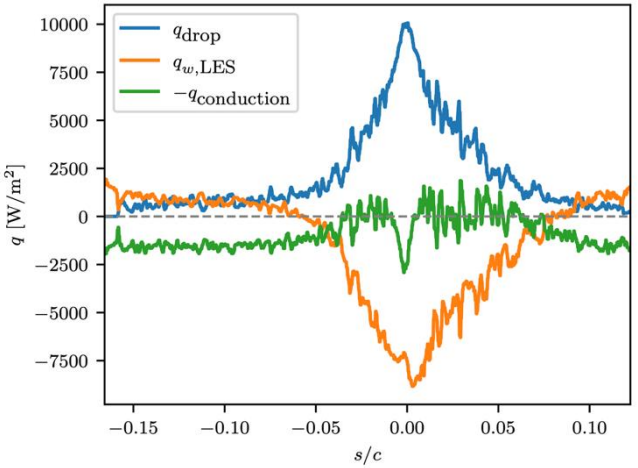


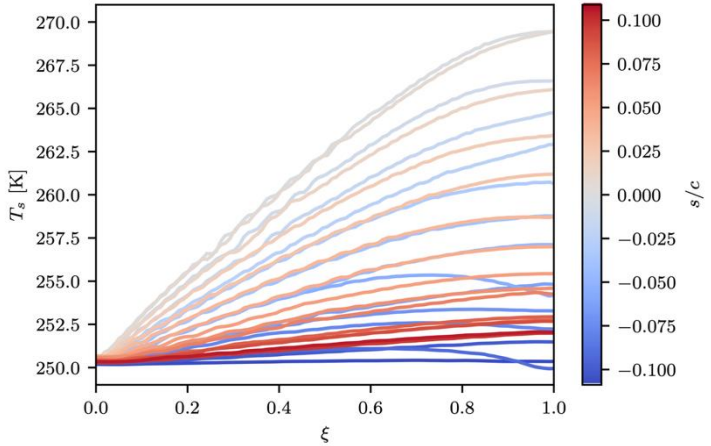
Energy balance at the interface

- Ice accretion is governed by the energy balance at the fluid-solid interface

$$q_{\text{drop}} + q_{w,\text{LES}} - q_{\text{conduction}} = 0$$

- At the stagnation line, q_{drop} is balanced by $q_{w,LES}$ (70%) and $q_{conduction}$ (30%).
- Downstream $q_{w,LES}$, changes sign, likely driven by the thermal boundary layer history effects.
- Near the airfoil skin, ice temperature profiles are linear. Near the ice surface, they exhibit significant curvature.





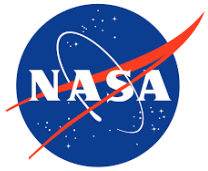
CTR Stanford University
CENTER FOR TURBULENCE RESEARCH

Conclusions

- We have presented a high-fidelity framework to simulate heat transfer in icing airfoils which couples WMLES (aero), Lagrangian tracking (droplets), and unsteady CHT (solid).
- Surface topology dictates local collection efficiency (β); windward peaks intercept higher droplet fluxes. This results in a highly heterogeneous surface heat source.
- Lateral conduction within the ice layer diffuses localized heat spikes. Resulting surface temperature field is significantly smoother than the impingement profile.
- Solid conduction is non-negligible and multidimensional near the leading-edge and around roughness elements.

Acknowledgments

- Thank you to the advisement and collaborations of Dr. Brett Bornhoft, Prof. Suhas Jain, Dr. Sanjeeb Bose, and Prof. Parviz Moin.
- The authors would like to acknowledge the funding provided by The Boeing Company, NASA's Transformational Tools and Technologies (TTT) Project.
- We would like to thank Prof. Stephen McClain, as well as Dr. Andy Broeren and Dr. Sam Lee of NASA Glenn for the experimental data and ice shapes.
- We acknowledge the generous computing resources Oak Ridge Leadership Computing Facility, which is a DOE Office of Science User Facility supported under Contract DE-AC0500OR22725.



OAK RIDGE National Laboratory | LEADERSHIP COMPUTING FACILITY

BOEING

CTR Stanford University
CENTER FOR TURBULENCE RESEARCH